Electrical Properties of Sand-Clay Mixtures Containing Trichloroethylene and Ethanol

J.J. Roberts, and D. Wildenschild

U.S. Department of Energy

Lawrence
Livermore
National
Laboratory

December 4, 2001

DISCLAIMER

This document was prepared as an account of work sponsored by an agency of the United States Government. Neither the United States Government nor the University of California nor any of their employees, makes any warranty, express or implied, or assumes any legal liability or responsibility for the accuracy, completeness, or usefulness of any information, apparatus, product, or process disclosed, or represents that its use would not infringe privately owned rights. Reference herein to any specific commercial product, process, or service by trade name, trademark, manufacturer, or otherwise, does not necessarily constitute or imply its endorsement, recommendation, or favoring by the United States Government or the University of California. The views and opinions of authors expressed herein do not necessarily state or reflect those of the United States Government or the University of California, and shall not be used for advertising or product endorsement purposes.

This is a preprint of a paper intended for publication in a journal or proceedings. Since changes may be made before publication, this preprint is made available with the understanding that it will not be cited or reproduced without the permission of the author.

This report has been reproduced directly from the best available copy.

Available electronically at http://www.doc.gov/bridge

Available for a processing fee to U.S. Department of Energy
And its contractors in paper from
U.S. Department of Energy
Office of Scientific and Technical Information
P.O. Box 62
Oak Ridge, TN 37831-0062
Telephone: (865) 576-8401
Facsimile: (865) 576-5728
E-mail: reports@adonis.osti.gov

Available for the sale to the public from
U.S. Department of Commerce
National Technical Information Service
5285 Port Royal Road
Springfield, VA 22161
Telephone: (800) 553-6847
Facsimile: (703) 605-6900
E-mail: orders@ntis.fedworld.gov
Online ordering: http://www.ntis.gov/ordering.htm

OR

Lawrence Livermore National Laboratory
Technical Information Department's Digital Library
http://www.llnl.gov/tid/Library.html

ELECTRICAL PROPERTIES OF SAND–CLAY MIXTURES CONTAINING TRICHLOROETHYLENE AND ETHANOL

Jeffery J. Roberts and Dorthe Wildenschild*
Lawrence Livermore National Laboratory, Livermore, CA 94551

*Now at Technical University of Denmark, Lyngby, Denmark

Abstract

A series of laboratory experiments, including the measurement of electrical properties and permeability, were performed on carefully characterized sand–clay mixtures. Different mixtures and configurations of quartz sand and 0 to 10% Na-montmorillonite clay were investigated using solutions of NaCl, $CaCl_2$, and deionized water. Samples containing 10% distributed clay were also studied using fluids containing 20 and 500 ppm trichlorethylene (TCE). Electrical properties were measured at frequencies between 10^6 and 10^{-2} Hz using the four-electrode method and Ag–AgCl inner electrodes on saturated samples at room temperature and 412 kPa confining pressure, corresponding to a soil depth of 15 to 20 m. Our results show that the addition of TCE has a small effect on electrical resistivity, with resistivity increasing with the addition of TCE. The influence of TCE on the electrical properties was most prominent in plots of loss tangent as a function of frequency. A loss tangent peak occurred at ~200 Hz. The height of the peak and the peak frequency both decrease with the addition of TCE. Further experiments were performed on samples containing a distinct clay layer parallel to current flow. Electrical properties were measured on water saturated samples and as a mixture of ethanol and water (80:20) was flowed through the sample. Resistivity increased by about a factor of four as the ethanol mixture replaced the water solution. Non-destructive x-ray imaging of the sample at various stages of dewatering indicates a decrease in the thickness of the clay layer with increasing number of pore volumes of ethanol–water flowed. Our results showed that electrical measurements are a useful tool for characterizing porous rocks and soils and that it is feasible to remotely detect the presence and follow the transport of contaminants such as TCE in the subsurface.

1. Introduction

1.1 Background

Electrical measurements are a useful non-destructive tool for characterization of porous rocks and soils. Conduction of electricity through porous media occurs primarily by movement of ions through the bulk saturating electrolyte. In addition, conduction takes place as adsorbed ions move along the surfaces of pores and cracks. Thus, the conductivity of a porous medium is related to microstructural properties such as porosity, pore geometry, and surface morphology of the mineral grains lining the pores, as well as the dielectric properties of the mineral grains and pore fluid. Electrical conduction is also a function of the prevailing fluid saturation. For brine-saturated porous materials Archie (1942) proposed the following relationship between bulk and fluid conductivities:

$$\rho_{bulk} = \rho_{fluid} a \varphi^m \qquad (1)$$

where ρ_{bulk} is the electrical conductivity of the porous medium, ρ_{fluid} is the electrical conductivity of the saturating fluid, φ is the porosity, and *a* and *m* are parameters that are supposed to be constant for a certain type of rock. The ratio ρ_{fluid}/ρ_{bulk} is the formation factor F. In equation (1) it is assumed that the contribution of surface conduction to the bulk conduction is negligible. When bulk conduction is important, Archie's law has to be modified (Johnson et al., 1986; Waxman and Smits, 1968; Sen et al., 1988; Sen and Goode, 1992). Instead of the pure proportionality between ρ_{bulk} and ρ_{fluid}, we obtain a linear dependence with an intercept on the ordinate axis. Johnson et al. (1986) defined a length parameter

Λ, which is a weighted volume-to-surface-area ratio (a measure of the dynamically interconnected pore size) defined as

$$\frac{\Lambda}{2} = \frac{\int |E(r)|^2 dV_p}{\int |E(r)|^2 dS} \tag{2}$$

E(r) is the electric potential field at point r, Vp is the pore volume and S is the surface area, i.e. the pore-solid interface. Λ is a parameter (with units of length) characteristic of the geometry of the porous medium and is thus transferable from one experiment to another for a specific medium. This relation is valid for materials where the (insulating) grains are coated with appreciable amounts of clay minerals (Johnson et al., 1986). When dry clays are saturated with brines the counter ions, which usually balance out charged impurities by bonding to their external surfaces, hydrate and become mobile within a layer. Surface conduction due to these counter ions then acts in parallel with the ionic conduction associated with the brine. For relatively high-salinity pore fluids, a linear relationship was derived (Johnson et al., 1986):

$$\rho_{bulk} = \frac{1}{F}\left(\rho_{fluid} + \frac{2\Sigma_s}{\Lambda}\right) \tag{3}$$

where Σ_s is the surface conductivity. When ρ_{fluid} and ρ_{bulk} are plotted on a linear scale, the slope equals the reciprocal of the formation factor F, and the intercept with the ordinate axis $b = 2\Sigma_s/F\Lambda$.

1.2 Previous Work

Previous work by Wildenschild et al., (1999, 2000) demonstrated the influence of various microstructural properties (such as clay content and configuration) on the electrical properties. They determined formation factors, Λ parameters, and surface conductances Σ_s for a number of different configurations containing 0 to 10 % clay. The arrangements included dispersed mixtures, discrete clay clusters and arrangements of distinct layers of clay in the sand matrix. They found the relationship (eqn. 3) suggested by Johnson et al. (1986) to describe conduction for a wide range of parameters including fluid salinity, clay content, and surface conductance. In this study we present additional work on samples studied by Wildenschild et al. (1999; 2000) using pore fluids that contain small amounts (<500 ppm) of TCE or ethanol/water mixtures.

Work on clay bearing materials containing organic compounds has been performed previously and some of this worked will be reviewed briefly here. Olhoeft and King (1991) reported complex resistivity measurements on synthetic clay-toluene mixtures. They found a resistivity increase (~10 to 30%) and a larger (negative) phase angle for samples containing up to 20% toluene. The resistivity difference was greatest at frequencies below ~100 Hz and the phase difference was greatest between 1 and 100 Hz. Work by Chan et al. (2000) on sand-clay mixtures shows that non-contaminated samples show little frequency dependence and follow Archie's law. When TCE was present in a 100% sand sample they found that Archie's law did not apply. Re-saturating the contaminated sample with brine produced anomalous results attributed to incomplete removal of TCE from the sample.

A comprehensive set of experiments on prepared and natural clay-bearing samples was performed by Jones (1997) as part of his thesis work. He measured complex electrical properties from 10^{-3} to 10^6 Hz while varying the solution type and concentration. Measurements were performed on samples containing a variety of organic contaminants including TCE, tetrachloroethylene, ethylene glycol, and phenol. Changes in the non-linear character of the complex electrical response were observed that were attributable to chemical reaction between the clay and the organic contaminants. Spectral alterations were observed to take place for as much as one month at which point equilibrium had not yet been established. These changes in non-linear response are suggested as a means of locating contaminated regions using field EM data.

2. Experimental Details

2.1 Sample Preparation and Characterization

We used a pure silica sand (F-50 Ottawa sand from U.S. Silica) and a Na-montmorillonite (Wyoming bentonite) to build the samples. The Ottawa sand has grain sizes between 74–420 microns, a median diameter (d_{50}) of 273 microns and a particle density of 2.66 g/cm^3. The samples were packed in 2-inch diameter heat shrink tubing with sintered Hasteloy frits at both ends that provided support, allowed fluid flow, and served as current electrodes. Sample height was 1.5 inches and AgCl coated silver wire electrodes were positioned in the casing 0.25 inches from either end of the sample using additional heat shrink material as spacing. The electrochemically coated Ag–AgCl wires served as potential electrodes. Platinum electrodes were unsuitable because of hydrolysis at the metal–water interface, causing unreliable measurements. The AgCl-coated wires alleviated this problem by providing a means of ionic exchange with the saturating solution.

Once the sand/clay was packed between frits the tubing was heated and would subsequently shrink to rigidly support the unconsolidated sample. The dispersed clay samples were packed from dry mixed sand and clay. In the case of the parallel sample, dry sand was packed around the vertical clay layer, which then was in contact with both end frits.

2.2 Pore Fluids

The samples were saturated with saline fluids of varying concentration, ranging from 0.0005 N to 0.75 N of CaCl$_2$ (0.05 to 64 mS/cm). Electrical measurements were also made using de-ionized water. Results are reported in Wildenschild et al. (2000). Solutions of 600 µS/cm NaCl (~0.0035 M) were prepared containing 0, 20, and 500 ppm TCE. These solutions were used as pore fluids in a 10% clay dispersed sample. The solubility limit for TCE in water at room temperature (20°C) is about 1099 ppm. Additional experiments were performed with an 80:20 mixture of ethanol and distilled water. This fluid was flowed through the sample containing a parallel clay layer.

3. Apparatus and Measurement Procedures

The experimental setup consists of 4 major components: the sample, the sample holder with pressure controls, the electrical measurement system, and the fluid flow system (Figure 1; Wildenschild et al., 2000). The sample is placed in a Hassler sleeve used to control pore pressure. The Hassler sleeve is placed between insulating Delrin end caps and is held in place by applied end-load and in-load pressures using air actuated cylinders. The various loads ensure that the sample is hydraulically sealed in the holder, i.e. sidewall flow is avoided and also provides for simulating shallow burial. We used end-load, in-load, and confining pressures of 60 psi (418 kPa) in all experiments. The end caps have openings for fluid inlet and outlet and for the electrical input and output voltage leads.
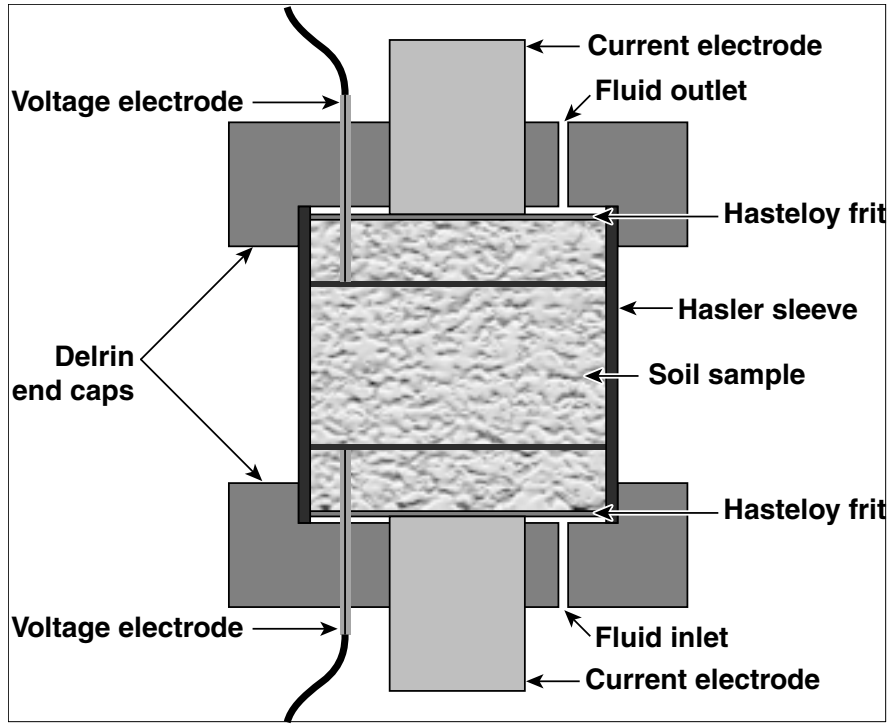
3.1 Electrical Measurements

As the various fluids were pumped through the samples, frequency-dependent electrical properties were measured using the four-electrode method (Olhoeft, 1985). Impedance magnitude, |Z|, phase angle ϕ, electrical resistance R, and capacitance C were measured with an HP4284A LCR meter during flow and at hydraulic equilibrium. Complex impedance spectra over a wider range of frequencies (10 mHz to 1 MHz) were measured using a Solartron 1260A impedance analyzer.

The complex impedance consists of a real and imaginary part and is given by

$$Z* = Z' - jZ'',$$
(4)

where Z' represents the real impedance, Z'' the imaginary impedance and $j = \sqrt{-1}$. The resistivity is the impedance, or resistance, taking into account the sample geometry

$$\rho* = Z*A/l.$$
(5)

Figure 1. Experimental apparatus for confining pressure, fluid flow, and impedance measurements.

Electrical conductivity σ is the reciprocal of the resistivity. The dielectric permittivity κ is related to the impedance by

$$\kappa^* = \kappa' - j\kappa'' = (j\omega C_0 Z^*)^{-1} \tag{6}$$

where κ^* is the dielectric permittivity divided by the permittivity of free space, ε_0, and has a value of 8.854×10^{-12} F/m, and C_0 is the capacitance of the empty cell in a vacuum ($C_0 = \varepsilon_0 A/l$). The loss tangent $\tan\delta$ is defined as

$$\tan\delta = \frac{\sigma' - \varepsilon''\omega}{\sigma'' + \varepsilon'\omega} \approx \frac{\sigma'}{\sigma''} \quad . \tag{7}$$

The loss tangent approximates the conductivity ratio for small angular frequency ω where conduction currents dominate displacement currents (Ward and Hohmann, 1987). The loss tangent is also called the dissipation factor and is a measure of the energy transferred to the material from the electric field, primarily through friction associated with the movement of ions and dipoles.

4. Results and Discussion

4.2 Electrical Measurements on Samples Containing TCE

The electrical impedance of the 10% dispersed bentonite sample changes with the amount of TCE present. Figure 2a plots the imaginary versus real impedance and shows an increase in the resistance with increasing TCE. Two impedance arcs are visible and both arcs widen, indicating a larger resistance, with an increase in the amount of TCE. Figure 2b shows the real and imaginary parts of the impedance plotted as a function of frequency. The critical frequency, the frequency where the minimum phase angle occurs (Dias, 2000), is lower by a factor of about 2.5 for the 500 ppm TCE sample compared to the clean sample. This is most readily observed in Figure 2a by noting where the imaginary impedance comes closest to the real axis.
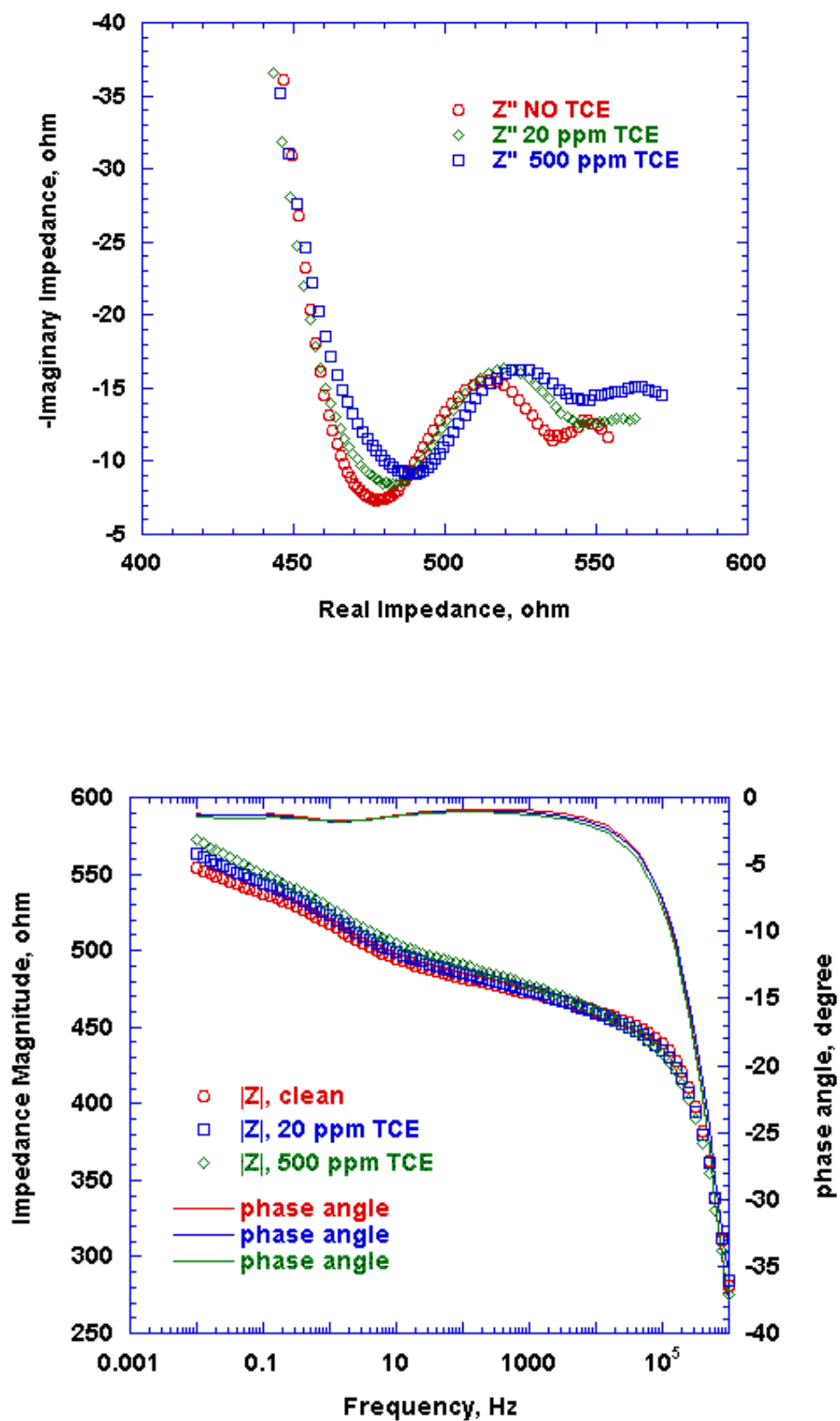
Figure 2. (a) Imaginary vs real impedance, (b) impedance magnitude and phase angle vs frequency.

The loss tangent for the three experiments is plotted in Figure 3. We found that the differences in electrical response are most apparent in this type of plot. The most prominent feature is the loss peak that occurs between 100 and 1000 Hz that decreases in magnitude and shifts to a slightly lower frequency with the addition of TCE. The frequency of the loss tangent peak coincides with the critical frequency.
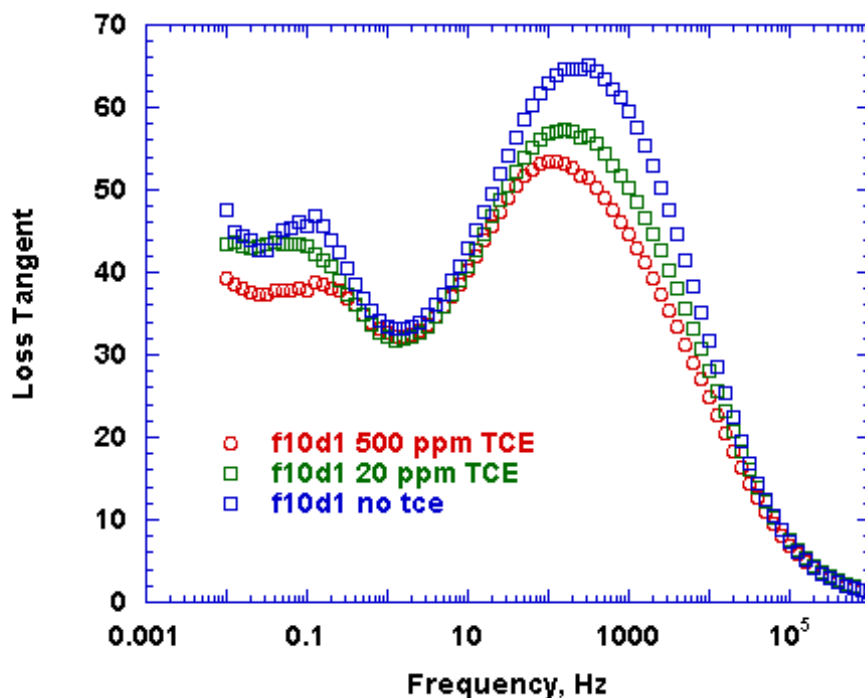
Figure 3. Loss tangent vs frequency for the three experiments.

The highest frequency impedance arc increases resistance about 5% for the 500 ppm TCE sample compared to the clean sample. Since TCE is a resistive fluid compared to the NaCl solution we expect an increase in resistance as the conductive fluid is displaced, but the change in resistance compared to the amount of TCE indicates an additional mechanism. The magnitude of the loss tangent peak decreases by about 17% with the addition of 500 ppm TCE. Possible contributors to this effect are a change in the exchangeability of the clay because of the TCE or other electrochemical reactions. Additional study is required to identify the cause. Nevertheless, it may be possible to use this information to locate small amounts of contamination in field sites using EM methods (Jones, 1997).

4.2 Electrical Measurements on Samples Containing Ethanol

Of interest in environmental remediation is the behavior of clay bearing soil that contains ethanol. Ethanol dewaters clays and causes them to contract. One problem with pump and treat remediation of clay-bearing soils containing organic contaminants is the amount of time it takes for the contaminant to diffuse to a permeable flow channel. One idea is that ethanol will not only dewater clay but cause microcracks in clay layers providing a shorter pathway for the migration and removal of contaminants. We have measured the electrical properties of a sand-clay sample containing a clay layer that is parallel to the direction of fluid flow and electrical measurement. Measurements were made using distilled water and $CaCl_2$ solutions ranging from 0.005 N to 0.4 N (Wildenschild et al., 2000) and as an 80:20

ethanol–water mixture was flowed through the sample at a rate of 5 mL/hour (the conductivity of the ethanol–water mixture is ~0.76 µS/cm).

The conductivity of the parallel clay sample increased as the salinity of the CaCl$_2$ fluid was increased, but not as strongly as other samples with 10% dispersed clay (Wildenschild et al., 2000). One reason for this is that the parallel clay sample had the highest surface conductance of all the types of samples studied (2.45 µS) and was fairly conductive even for the most dilute solutions. The loss tangent for the dispersed-clay experiments displays more variation than the loss tangent for the parallel-clay layer samples (Figure 4a and b). The loss tangent for the dispersed-clay sample increases with increasing salinity and shows more peaks or peaks shifted to lower frequency. These low frequency peaks occur between 110 and 0.1 Hz and are absent for the samples saturated with distilled water and the ethanol–water mixture.

As the ethanol mixture was flowed through the sample the impedance increased by about a factor of 4 over the 0.022 N CaCl$_2$ solution impedance. Additional flow of the ethanol–water mixture to up to 10 pore volumes continued to increase the impedance. After 15 pore volumes the fluid flow was stopped and impedance decreased with time. The loss tangent shows a single peak centered near 500 Hz for the ethanol–water saturated sample. With additional flow the peak first becomes lower in magnitude then increases. After about 10 pore volumes have been displaced a second peak or shoulder appears at higher frequency. The noisiness of the response increases with time.
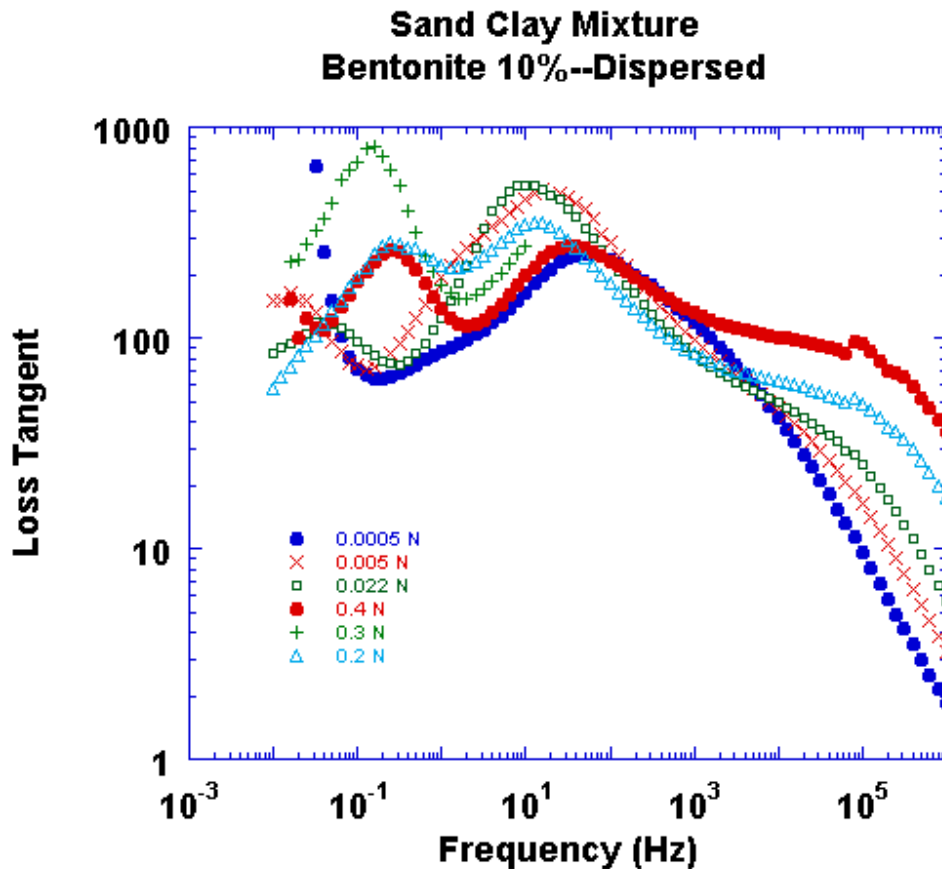

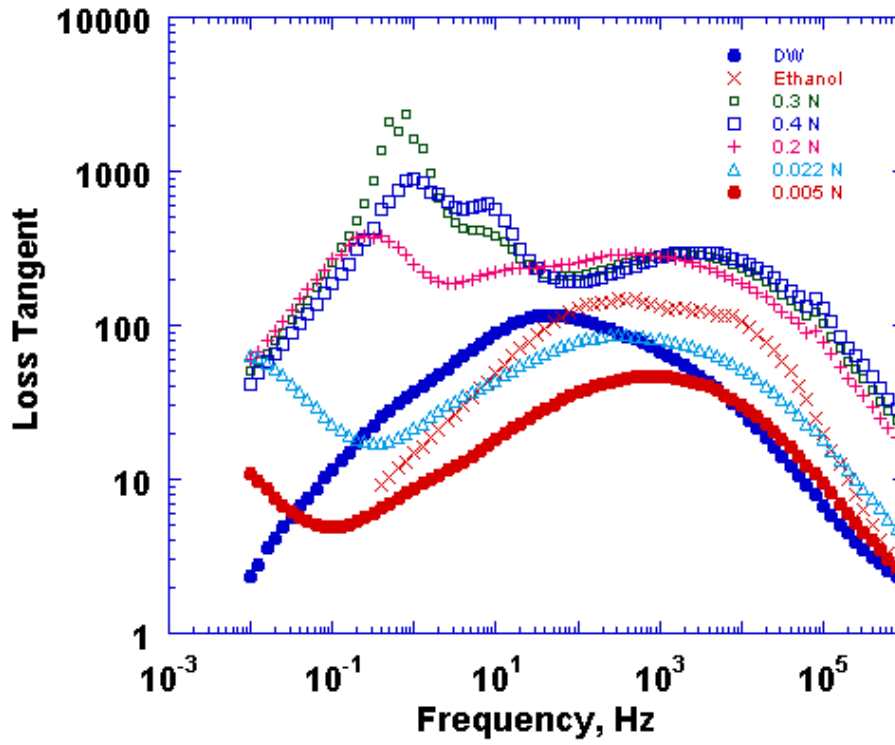**Figure 4. (a) Loss tangent vs frequency for dispersed-clay experiment.**

Figure 4. (b) Loss tangent vs frequency for parallel-clay experiment.

4.3 X-Ray Images

The parallel clay layer sample was x-rayed periodically during the ethanol–water flow portion of the experiment. Flow was stopped periodically and the sample was x-rayed to gain information about the thickness and integrity of the clay layer. The x-ray procedure is very similar to that described by Roberts and Lin (1997). A 160 kVp linear source was used as the sample was rotated and translated vertically through the beam. A two-dimensional photo-diode linear array detector was used to convert and store the digital signal. The independent views (radiographs) were reconstructed into a series of tomographic slices. The information obtained is the attenuation of the sample as a function of time. Spatial resolution for this system was about 390 μm, although other systems in our laboratory can achieve spatial resolutions down to about 20 μm. Higher resolution scans will be required to image microcracks in the clay layer.

Reconstructed tomographic cross sections of the cylindrical sample are shown in Fig. 5a and 5b. In these gray-scale images a brighter shade is more attenuating than a darker shade. Figure 5a shows the sample prior to ethanol–water flow and Figure 5b shows the sample after ~10 pore volumes of 80:20 ethanol–water have flowed through the sample. The samples are ~5.08 cm diameter and each pixel is ~390 μm × 390 μm. The primary feature to note is the thickness of the clay layer (gray vertical stripe in the center of the images) before and after flow. Although the spatial resolution of these images is insufficient to image cracking in the clay, it is easy to see the effect of dewatering.
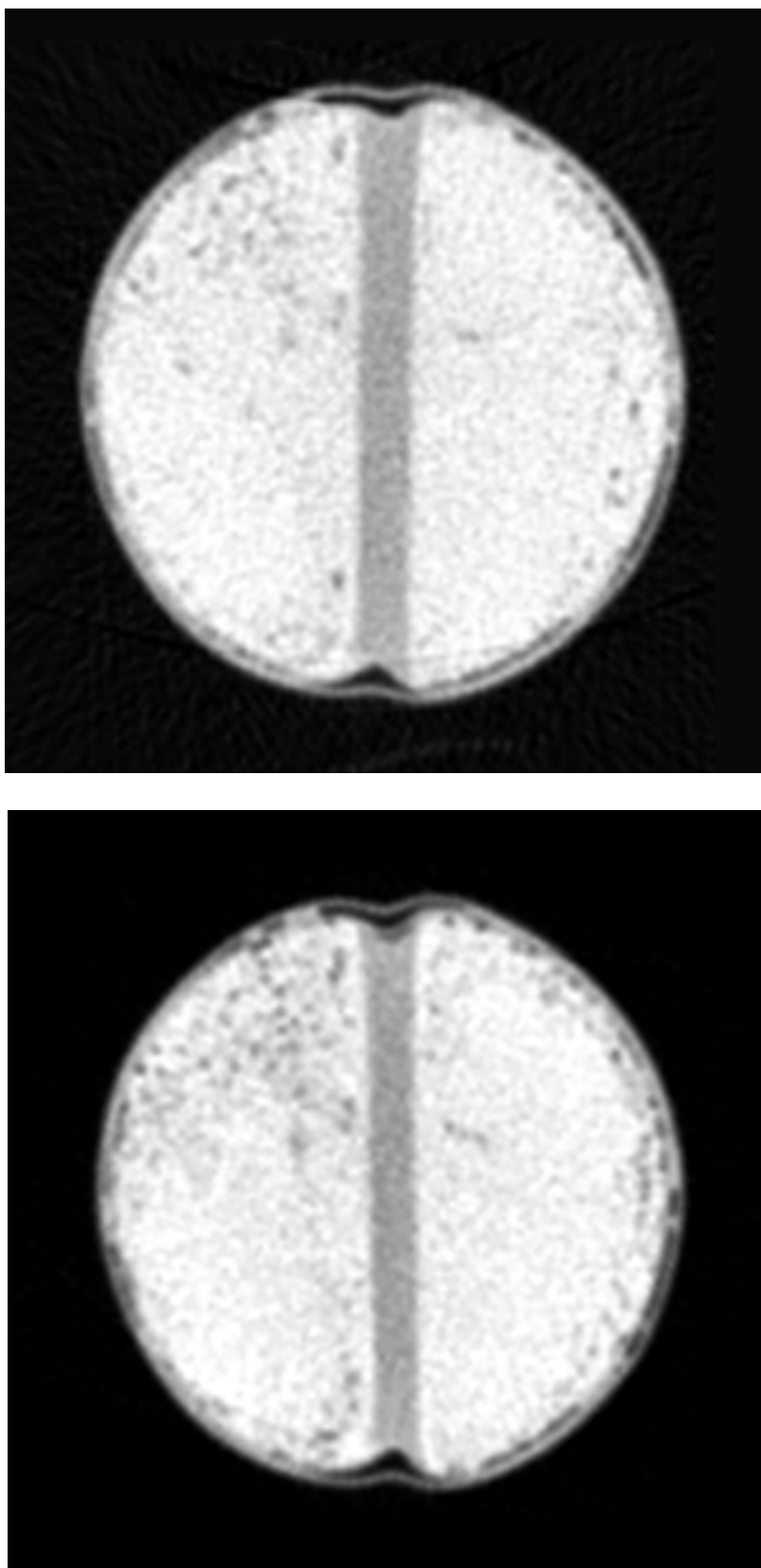
Figure 5. Reconstructed x-ray CT slices of the parallel clay layer sample (a) prior to ethanol–water flow and (b) after ~10 pore volumes of flow. Sample is ~5.04 cm in diameter.

Figures 6a and 6b show averaged lines of attenuation across the clay layer (Fig. 6a, horizontal) and within the clay layer (Fig. 6b, vertical). Five lines were averaged for smoothing of data. The axes are distance and relative attenuation units. The curves are labeled sequentially from early in the experiment to later in the experiment and correlate to the amount of ethanol that has flowed through the sample. In Fig. 6a we see the width of the clay layer getting smaller and in Fig. 6b we see the attenuation of the clay layer increasing with time and total flow. The thickness of the clay layer has changed by 25-40% with approximately ten pore volumes of fluid flow.
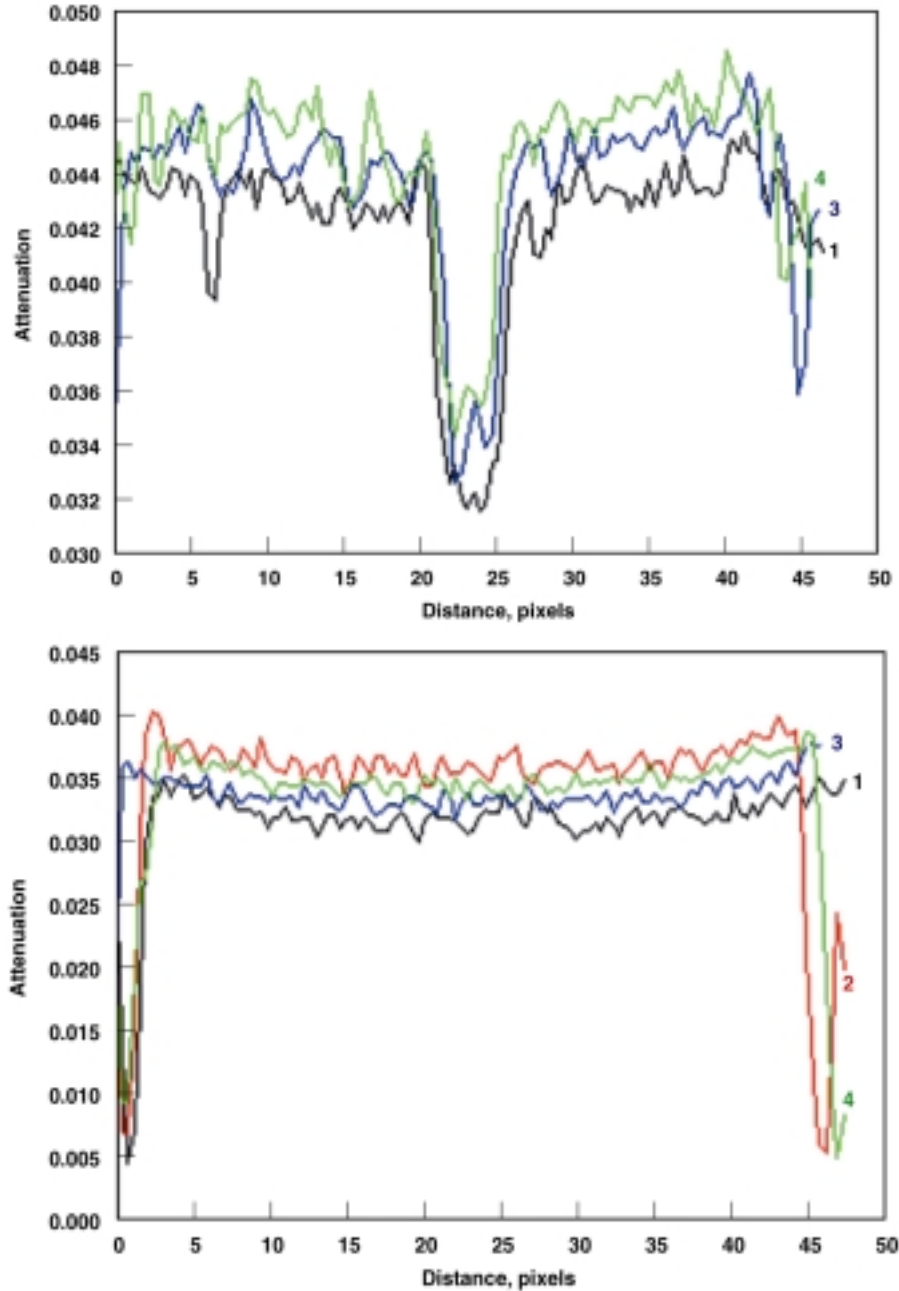
Figure 6. Relative attenuation vs distance across sample as a function of total flow and time for the parallel-clay layer sample using 80:20 ethanol–water as the pore fluid.
(a) Attenuation across the clay layer indicates a shrinking layer with time and flow.
(b) Attenuation within the clay layer shows increased attenuation with time and total flow.

5. Conclusions

We have investigated the influence of 20 to 500 ppm TCE on the complex impedance of sand-clay samples. The presence of TCE had only a minor effect on the electrical resistivity. A more pronounced effect was observed in the loss tangent with a peak centered near 200 Hz that shifts to slightly lower frequency and decreases in height with the addition of TCE. Electrical experiments were performed on a sample containing a parallel clay layer while an ethanol–water mixture was displaced through the sample. Resistivity increased by as much as a factor of four as the ethanol–water mixture replaced the 0.022 N $CaCl_2$ solution. X-ray imaging during the dewatering experiment quantified the change in the clay layer which decreased in thickness by ~33% with about 10 pore volumes of ethanol–water mixture flowed. Additional analyses using a higher spatial resolution x-ray system is needed to determine the presence and extent of microcracking in the clay due to dewatering.

6. Acknowledgements

7. References

Archie, G.E. (1942), "The Electrical Resistivity Log as an Aid in Determining Some Reservoir Characteristics," *Trans. AIME*, 146, 54-62.

Chan, C. Y., H. M. Buettner, R. Newmark, and G. Mavko (2000), "Conductivity Measurements of Sand-Clay Mixtures: A Modified Experimental Method," *J. Env. and Engin. Geophys., 5*, 15-26.

Dias, C. A. (2000), "Developments in a Model to Describe Low-Frequency Electrical Polarization of Rocks," *Geophysics, 65*, 437-451.

Glover, P.W.J., P.G. Meredith, P.R. Sammonds, and S.A.F. Murrell (1994), "Ionic Surface Electrical Conductivity in Sandstone," *J. Geophys. Res.*, 99, 21635-21650.

Johnson, D.L., J. Koplik, and L.M. Schwartz (1986), "New Pore-Size Parameter Characterizing Transport In Porous Media," *Phys. Rev. Lett*, 57, 2564-2567.

Jones, D. P. (1997), "Investigation of Clay-Organic Reactions Using Complex Resistivity," Ph.D. thesis, Colorado School of Mines.

Kostek, S., L.M. Schwartz, and D.L. Johnson (1992), "Fluid Permeability In Porous Media: Comparison Of Electrical Estimates With Hydrodynamical Calculations," *Phys. Rev. B*, 45,186-195.

Olhoeft, G.R. (1985), "Low-Frequency Electrical Properties," *Geophysics*, 50, 2492-2503.

Olhoeft, G. R. and T. V. V. King (1991), Mapping Subsurface Organic Compounds Noninvasively By Their Reactions With Clays, USGS Water Resources Investigation Report 91-4034.

Roberts, J. J., and W. Lin (1997), "X-Ray Radiography of Fracture Flow and Matrix Imbibition in Topopah Spring Tuff Under a Thermal Gradient," *Int. J. Rock Mech. & Min. Sci.,* 34:3-4, Paper No. 259.

Sen, P.N. and P.A. Goode (1992), "Influence of Temperature on Electrical Conductivity on Shaly Sands," *Geophysics*, 57, 89-96.

Sen, P.N., P.A. Goode, and A. Sibbit (1988), "Electrical Conduction In Clay Bearing Sandstones At Low And High Salinities," *J. Appl. Phys.*, 63, 4832-4840.

Ward, S. H., and G. W. Hohmann (1987), "Electromagnetic Theory for Geophysical Applications," in *Electromagnetic Methods in Applied Geophysics*, vol. 1, M. Nabighain, ed., Society for Exploration Geophysics, pp. 131-311.

Waxman, M.H. and L.J.M. Smits (1968), "Electrical Conductivities In Oil-Bearing Shaly Sands," *Soc. Pet. Eng. J., 8*, 107-122.

Wildenschild, D., J. J. Roberts, and E. D. Carlberg (1999), "Influence of Microstructural Properties on Geophysical Measurements in Sand-Clay Mixtures," *Symposium on the Application of Geophysics to Engineering and Environmental Problems*.

Wildenschild, D., J. J. Roberts and E. D. Carlberg (2000), "Electrical Properties of Sand-Clay Mixtures: The Effect of Microstructure," *Geophys. Res. Lett.*, 27, 3085-3089.